

Nuclear Structure Effects in ($p, 2$ nucleon) Reactions on the Separated Isotopes of Tellurium at 300 MeV*†

Roy F. Schall, Jr.,‡ and Albert A. Caretto, Jr.

Department of Chemistry, Carnegie-Mellon University, Pittsburgh, Pennsylvania 15213

(Received 12 June 1970)

The cross sections of ($p, 2p$), (p, pn), and ($p, 2n$) reactions at 300 MeV on the separated isotopes of tellurium were determined. The total (p, pn) cross sections, for those cases in which it was only possible to measure one of the isomeric states in the product, was calculated by assuming that the direct knockout mechanism was predominant. Both the total (p, pn) cross sections and the ($p, 2n$) cross sections are directly proportional to the neutron skin thickness. This is consistent with the assumption that these reactions take place by direct knockout processes in the diffuse or peripheral region of the nucleus. The tellurium ($p, 2p$) reactions were observed to be inversely proportional to the neutron skin thickness.

INTRODUCTION

The objectives of this study are identical to those indicated for the preceding paper.¹ The cross sections of ($p, 2$ nucleon) reactions, at 300 MeV, were measured for as many of the target-product systems as practical using the enriched separated isotopes of tellurium as targets. In particular tellurium targets of ¹²²Te to ¹³⁰Te were employed.

This work, together with the results reported for the separated cadmium isotope targets,¹ constitute the only two detailed studies of the dependence of ($p, 2n$), (p, pn), and ($p, 2p$) reaction cross sections on target nuclear composition spanning an extended mass region.

The various mechanisms that have been postulated for ($p, 2$ nucleon) reactions were described in the preceding paper.¹ An objective of this study is to examine the extent of agreement of these results with predictions based on these various mechanisms. Furthermore, it is of interest to make comparisons of the results of these two separated-isotope target systems.

EXPERIMENTAL

All isotopes of tellurium, except ¹²⁰Te, were obtained as maximum enrichment elemental powders from the Isotopes Development Center of the Oak Ridge National Laboratory. ¹²⁰Te was not available as a sufficiently enriched isotope to be useful as a target. Table I lists the target isotopes and their enrichments. These powders were mixed with 99.99% pure aluminum powder to obtain a tellurium concentration of ~1% and pressed with a hydraulic press into self-supporting target pellets 2 cm × 1.5 cm in area. The pellet weights were less than 230 mg in all cases. On each side of the target pellet was placed a ½-mil guard foil, a 1-mil beam monitor foil, and a 1.2-mil product-nucleus

recoil catcher foil, each cut from 99.99% pure aluminum foil. Irradiations were carried out in the internal circulating beam of the Carnegie-Mellon University proton synchrocyclotron at a radial distance corresponding to 300 ± 13 MeV. The lengths of bombardment were kept short with respect to the half-lives of the radioactivities sought for a particular run, and ranged from 5 min to 2 h. The target pellet and foils were mounted for bombardment using a jig to insure good leading edge and side alignment. An assessment of the alignment was made on each run by comparing the ²⁴Na counting rates in the upstream and downstream monitor foils. In all cases the difference in ²⁴Na activity in these foils was 3% or less. Following the irradiations the target stack was separated. The beam monitor foils were set aside for the ²⁴Na activity determination, the guard foils were discarded, and the catcher foils and target pellet dissolved for chemical purification of the desired products by standard techniques.² All chemical yields were determined gravimetrically: tellurium as elemental, antimony as metal, and iodine as PdI₂.

TABLE I. Target element isotopic purity. Analyses provided by Oak Ridge National Laboratory.

	122	123	124	125	126	128	130
	(%)						
¹²² Te	94.8	0.53	0.65	0.61	1.11	1.21	1.12
¹²³ Te	2.0	76.5	7.3	3.1	4.8	3.7	2.7
¹²⁴ Te	0.5	0.6	93.9	1.7	1.4	1.1	0.8
¹²⁵ Te	0.1	0.1	0.36	95.56	2.60	2.04	0.44
¹²⁶ Te	0.02	0.02	0.05	0.20	98.69	0.81	0.24
¹²⁸ Te	0.05	0.05	0.05	0.05	0.06	99.46	0.48
¹³⁰ Te	0.04	0.02	0.02	0.03	0.1	0.3	99.49
	0.03	0.02	0.03	0.02	0.1	0.33	99.5

TABLE II. Nuclides used in this study. (Data taken from Ref. 3.)

	Half-life <i>et al</i>	Radiation detected	<i>E</i> max (MeV)	Branching ratio
¹²² Sb	2.80 day	β-	1.97	0.97
¹²⁴ Sb	60.4 day	β-	2.31	1.00
¹²⁵ Sb	2.71 yr	β-	0.61	1.00
¹²⁷ Sb	93 h	β-	1.5	1.00
¹²⁹ Sb	4.3 h	β-	1.87	1.00
^{121g} Te	17 day	x	0.026	1.00
^{123m} Te	117 day	γ	0.16	1.00
^{125m} Te	58 day	x	0.027	1.00 (Te x rays)
^{127g} Te	9.4 h	β-	0.70	0.997
		β-	0.027	0.003
^{127m} Te	109 day	β-	0.70	0.992 (^{127g} Te)
		β-	0.72	0.008
^{129g} Te	69 min	β-	1.45	1.00
^{129m} Te	34 day	β-	1.45	0.64 (^{129g} Te)
		β-	1.59	0.30
		β-	1.56	0.06
¹²¹ I	2.12 h	x	0.027	0.91
¹²³ I	13.3 h	x	0.027	1.00
¹²⁴ I	4.15 day	x	0.027	0.74
¹²⁵ I	60.2 day	x	0.027	1.00

The tellurium 127 and 129 isomers, and all anti-mony product β radiations, were detected by end-window methane-flow proportional counters. The ^{125m}Te and ^{121g}Te x rays from internal-conversion deexcitation and electron capture, respectively, were counted on 1-in. × $\frac{1}{32}$ -in. thick NaI(Tl) x-ray scintillation crystals. The ^{123m}Te γ rays were measured on a 3-in. × 3-in. γ-scintillation detector. Least-squares fits of the various component activities, obtained by computer analysis of the counting data, were extrapolated to end of bombardment and were used to calculate cross sections. Table II gives decay data³ used for this study. The chemical separations were performed sufficiently fast to minimize contributions to any yield from known isobaric decay. However, the value for the ¹²⁵Te(*p*, 2*p*)¹²⁴Sb is probably low be-

cause of β decay of the first excited state of ¹²⁴Sb prior to chemical separation. All cross sections were corrected for minor contributions to the product activities from more complicated reactions than the (*p*, 2 nucleon) reactions resulting from impurity tellurium isotopes in the targets (see Table I). These corrections were either based on measurements made in this study, or on cross-section values or estimates based on identical or similar reactions reported in the literature.⁴⁻⁷

RESULTS

The experimentally determined (*p*, 2 nucleon) reaction cross sections of 300-MeV protons incident on the various separated tellurium targets are listed in Table III. The uncertainties indicated are rms deviations from the average for replicate determinations. Most of the systematic uncertainties are about the same as for the previously reported separated cadmium isotope studies. An estimate of the uncertainties of many of the individual experimental measurements involved in these cross-section determinations are listed in Table IV. In spite of these total uncertainties, the best accuracy to be anticipated for radiochemical studies of this type is about ±20%.⁸

Except for the case of ¹²³Te, corrections to the measured (*p*, 2 nucleon) cross section from possibly more complicated reactions on target impurities were small. No correction was applied for the possible effect of secondary particles producing the reaction product. Measurements by others^{1,9} on the dependence of the (*p*, 2 nucleon) cross section on target mass has indicated no noticeable effect for target thickness between about 10 to 200 mg/cm². The targets used in this work were always less dense than about 120 mg/cm². However, measurements do not exist for the possible effect of secondaries for thicknesses less than 10 mg/cm², and, thus, an error may exist but its value cannot be estimated.

TABLE III. Experimental and calculated cross sections at 300 MeV (mb).

Target	<i>(p</i> , 2 <i>n</i>)	<i>(p</i> , 2 <i>p</i>)	Meta state	<i>(p</i> , <i>pn</i>)		Total	Calculated total <i>(p</i> , <i>pn</i>)
				Ground state	Isomeric ratio (m/g)		
¹²² Te	3.73 ± 0.75	19.7 ± 4.9	34.0
¹²³ Te	...	11.8 ± 1.9
¹²⁴ Te	5.3 ± 2.1	...	15.7 ± 4.4	41.1
¹²⁵ Te	4.41 ± 0.26	6.39 ± 1.54
¹²⁶ Te	6.3 ± 1.7	7.80 ± 2.10	17.7 ± 1.8	40.0
¹²⁸ Te	...	5.43 ± 0.87	19.4 ± 2.0	27.5 ± 4.2	0.71	46.9 ± 8.8	44.3
¹³⁰ Te	...	5.84 ± 0.82	23.2 ± 3.1	30.2 ± 1.1	0.78	53.4 ± 6.8	52.7

TABLE IV. Experimental measurement uncertainties involved in cross-section determination.

Measurement	Estimate of uncertainty (%)
$^{27}\text{Al}(p, 3pn)^{24}\text{Na}$ monitor cross section	6.5
Beam on and off times and constancy of beam intensity	5.5
Target weights	0.5
Separated isotope weights	0.1
Leading edge alignment	2.0
Pipetting errors	2.0
Counting errors (long term)	3.0
Chemical yields	2.0
Carrier concentration	2.0
Decay-curve analysis	5.0
Half-life errors	0.1 - 6.0 ^a
Source activity purity	0 - 20 ^a
Total systematic uncertainty	13 - 26 ^a

^aDepends on particular nuclide. See Ref. 2 for specific details.

DISCUSSION

A. (p, pn) Reactions

Except for ^{128}Te and ^{130}Te , the cross sections listed in Table III for the (p, pn) reactions on the lighter tellurium nuclides are for either the upper or lower isomeric state. The isomeric ratios for the $^{128}\text{Te}(p, pn)^{127}\text{Te}$ and $^{130}\text{Te}(p, pn)^{129}\text{Te}$ were measured in this work and can be compared with other values in the literature. Gatrousis¹⁰ has reported for the $^{128}\text{Te}(p, pn)^{127}\text{Te}$ isomeric ratio a value of 0.71 at 40 MeV and a value of 0.81 at 150 MeV. For the $^{130}\text{Te}(p, pn)^{129}\text{Te}$ isomeric ratio Maurer and Wiig¹¹ report a value of 0.83 at 233 MeV, and Gatrousis¹⁰ reports a value of 0.68 at 150 MeV. The present work at 300 MeV, indicates

a value of the $^{128}\text{Te}(p, pn)^{127}\text{Te}$ isomeric ratio of 0.71 and for $^{130}\text{Te}(p, pn)^{129}\text{Te}$ a value of 0.77.

Assuming these reactions, at 300 MeV, take place predominately by knockout processes, it is possible to estimate the isomeric ratio predicted by this mechanism. Using shell-model states with binding energies up to 10 MeV as given by Ross, Mark, and Lawson,¹² and making use of the fractional neutron availability factors calculated by Benioff,¹³ the isomeric ratio was calculated for each of the tellurium target nuclides. The fractional neutron availabilities M_N calculated by Benioff at 5.7 GeV are doubtlessly in error for 300-MeV protons. However, since they enter into these calculations as a ratio, the error may be partially cancelled. The calculation assumes that neutron-hole states, produced in any of the shell-

TABLE V. Calculation of Te(p, pn) isomeric ratios.

	Neutron availabilities (Ref.12)	Tellurium targets					
		^{122}Te	^{124}Te	^{126}Te	^{128}Te	^{130}Te	
		Neutron occupation numbers					
Shell-model levels	$2d_{3/2}$	0.127	2	4	4	4	4
	$1h_{11/2}$	0.135	2	2	4	6	8
	$3s_{1/2}$	0.145	2	2	2	2	2
	$2d_{5/2}$	0.127	6	6	6	6	6
	$1g_{7/2}$	0.087	8	8	8	8	8
Calculated isomeric ratio			0.74	0.62	0.79	0.77	0.75
Experimental isomeric ratio						0.71	0.78

model states indicated, deexcite by a minimum number of quadrupole γ transitions to either the $\frac{1}{2}^+$ or $\frac{3}{2}^+$ ground states or the $\frac{1}{2}^-$ excited state of the (p, pn) product nuclides. Hole states produced exactly between the ground state and excited state are assumed to branch equally to these states in deexcitation. The parameters assumed and the results obtained in these calculations are listed in Table V. It should be noted that good agreement with the experimental values was obtained for the ^{128}Te and ^{130}Te targets, which tends to provide confidence in the isomeric ratios calculated for the other cases. Using these ratios, the total (p, pn) cross section for all the tellurium isotopes was calculated and is listed in column eight in Table III.

As was suggested in the previous paper¹ for the cadmium (p, pn) reactions, as well as by others,¹⁴ the (p, pn) reaction for a series of isotopes should be dependent on the thickness of the neutron skin in the periphery of the nucleus. Quasifree scattering experimental data,¹⁵ as well as theoretical¹² and Monte Carlo calculations,¹⁶ indicate that most of the nucleon-nucleon interactions which successfully lead to ($p, 2$ nucleon) products take place in the peripheral region of the nucleus. The composition of this region, as perhaps given by the neutron skin thickness, should effect the probability of (p, pn) reactions. Making use of the relations given by Myers,^{17,18} based on a refinement of the liquid-drop model, the neutron skin thickness was calculated for each of the tellurium isotope targets.

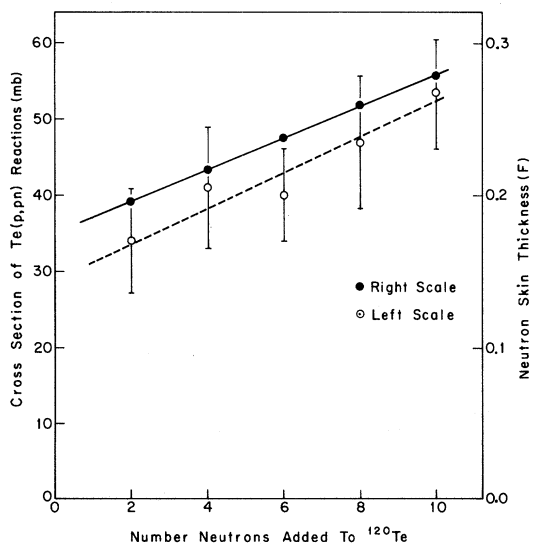


FIG. 1. Cross section of $\text{Te}(p, pn)$ reactions and target isotope neutron skin thickness (in F) versus the number of neutrons in the target above ^{120}Te . \circ experimental cross-section data, \bullet calculated neutron skin thickness (see Ref. 16).

These values and the (p, pn) cross sections are plotted in Fig. 1. The striking similarity of the dependence of each of these curves on neutron number is consistent with the conclusion that these (p, pn) reactions take place predominately by knockout processes in the peripheral or skin region of the nucleus.

B. ($p, 2p$) Reactions

Figure 2 is a plot of most of the cross sections of ($p, 2p$) reactions available in the literature, versus target mass number for proton energies between 300 and 400 MeV.¹⁹⁻²⁵ Included in this figure are tellurium and cadmium results reported here and in the preceding paper. Disregarding the values for the tellurium targets, most of the cross sections appear to fall between about 12 and 24 mb (dashed lines in Fig. 2). Both the cadmium and the tellurium ($p, 2p$) cross sections decrease with increasing neutron number. The only abnormally high value is for ^{58}Ni . It is interesting to note that ^{58}Ni has a filled $1f_{7/2}$ proton shell, all of which is probably available for ($p, 2p$) reactions. Furthermore ^{68}Zn , which has two protons above the filled $1f_{7/2}$ shell, has only about 62% of the ^{58}Ni cross section. A similar situation appears to be present at tellurium, which has two protons above the filled $1g_{9/2}$ proton shell, and as a group, have cross sections about 20-50% lower than the corresponding cadmium targets which are only two protons short of having a filled $1g_{9/2}$ level.

The dependence of the tellurium ($p, 2p$) cross sections on neutron skin thickness is illustrated in Fig. 3. Also illustrated, for comparison purposes, are the values for the cadmium targets. It is clear that as the peripheral region of the nucleus becomes more neutron rich the probability for ($p, 2p$) reactions decreases.

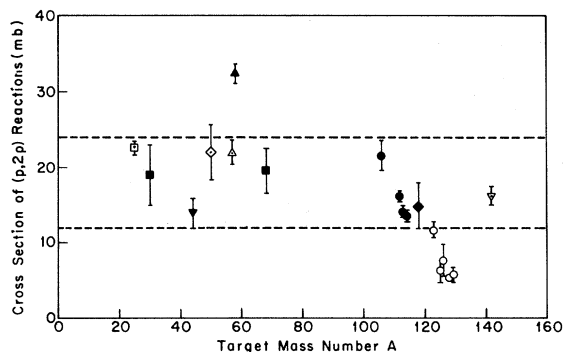


FIG. 2. Cross section of ($p, 2p$) reactions between 300 and 400 MeV versus target mass number. \circ this work; \bullet Ref. 1; \square Ref. 18; \blacksquare Ref. 19; \blacktriangledown Ref. 20; \diamond Ref. 13; \triangle Ref. 21; \blacktriangle Ref. 22; ∇ Ref. 23; \blacklozenge Ref. 24.

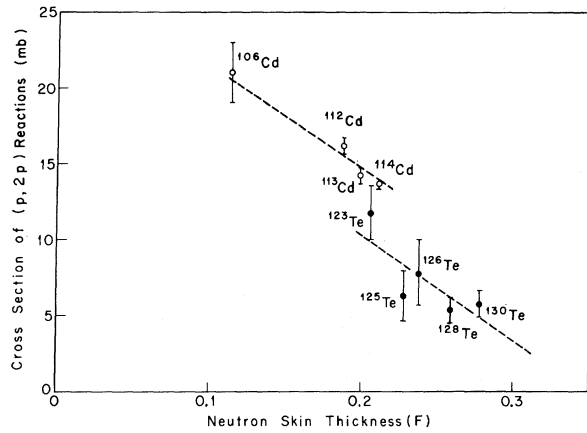


FIG. 3. Dependence of tellurium and cadmium ($p, 2p$) reaction cross sections on neutron skin thickness.

C. ($p, 2n$) Reactions

The tellurium and cadmium ($p, 2n$) reactions are plotted versus neutron skin thickness in Fig. 4. As in the case of the (p, pn) reactions a correlation with skin thickness is observed although the scatter is somewhat worse. These reactions probably involve a p - n charge-exchange scattering followed by neutron evaporation. For a ($p, 2n$) reaction these charge-exchange scatterings are restricted to those scattering angles consistent with the deposition of from about 10 to 20 MeV of excitation energy. If these nucleon-nucleon interactions take place at locations deep within the nucleus the effects of attenuation and refraction would increase the probability that the initial interaction would lead to other nucleon-nucleon scatterings. Thus, the most probable location for the initial interaction, if it is to be limited to one charge-exchange scattering, is in the peripheral region of the nucleus. The probability for p - n interactions in this region should be related to the neutron skin thickness. It is therefore consistent with this mechanism that the over-all trend of ($p, 2n$) reaction cross sections, for fixed Z , be dependent on the neutron skin thickness. The fact that ^{108}Cd does not adhere to this trend may be related to differences in level densities or binding energies which control the evaporation step.

CONCLUSIONS

Both (p, pn) and ($p, 2n$) reaction cross sections appear to be directly proportional to the neutron

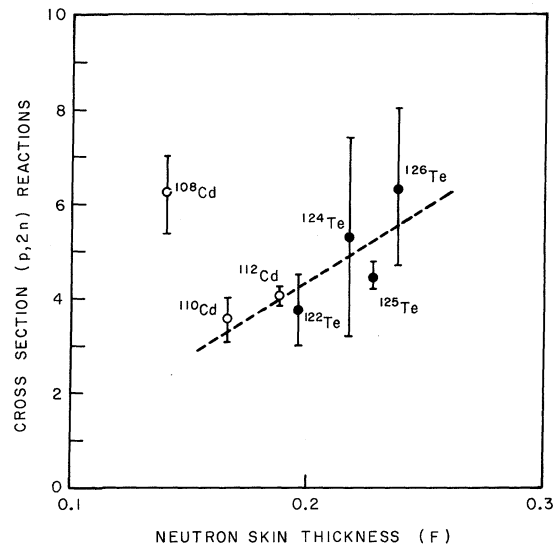


FIG. 4. Dependence of tellurium and cadmium ($p, 2n$) reaction cross sections on neutron skin thickness. \circ cadmium data, Ref. 1; \bullet tellurium data, this work.

skin thickness of the target nucleus. The fact that the ($p, 2n$) reaction is also sensitive to this quantity would imply that both one-step processes, such as those taking place by direct knockout, and two-step processes such as inelastic scattering followed by nucleon evaporation or charge-exchange scattering followed by nucleon evaporation are all dependent on the nature of the peripheral region of the nucleus. As the radius of the neutron density distribution extends beyond the radius of the proton density distribution, the probability of simple proton-neutron interactions increases, while that of proton-proton interactions decreases. This is borne out by the decrease in the ($p, 2p$) reaction cross sections with increasing neutron skin thickness.

ACKNOWLEDGMENTS

We wish to thank the operating staff of the Carnegie-Mellon University Nuclear Research Center for aid in making the irradiations. We also appreciate the assistance of Mrs. Carol Kier and Gary Smay in sample counting and other miscellaneous help. We also extend our appreciation to John Urbon for performing some of the computer calculations on relative evaporation probabilities.

*Research performed under a contract with the U. S. Atomic Energy Commission.

†Presented in partial fulfillment of the requirements of the Ph.D. degree in the Department of Chemistry, Carnegie Institute of Technology, Pittsburgh, Pennsylvania 15213.

‡Present address: Health Physics Section, Walter Reed Army Medical Center, Washington, D. C. 20012.

¹W. J. Nieckarz, Jr., and A. A. Caretto, Jr., preceding paper [Phys. Rev. C **2**, 1917 (1970)].

²R. F. Schall, Jr., Ph.D. thesis, Carnegie Institute of Technology, 1968 (unpublished).

³C. M. Lederer, J. M. Hollander, and I. Perlman, *Table of Isotopes* (John Wiley & Sons, Inc., New York, 1967), 6th ed.

⁴N. T. Porile, Phys. Rev. **125**, 1379 (1962).

⁵D. R. Nethaway and L. Winsberg, Phys. Rev. **119**, 1375 (1960).

⁶J. A. Panontin, N. T. Porile, and A. A. Caretto, Jr., Phys. Rev. **165**, 1273 (1968).

⁷W. J. Treytl and A. A. Caretto, Jr., Phys. Rev. **146**, 836 (1966).

⁸J. M. Miller and J. Hudis, Ann. Rev. Nucl. Sci. **9**, 51 (1959).

⁹L. B. Church and A. A. Caretto, Jr., Phys. Rev. **178**, 1732 (1969).

¹⁰C. Gatrousis, Clark University Annual Progress Report, 1964, p. 7.

¹¹D. W. Maurer and E. O. Wiig, J. Am. Chem. Soc. **84**, 4059 (1962).

¹²A. A. Ross, H. Mark, and R. D. Lawson, Phys. Rev. **102**, 1613 (1956).

¹³P. A. Benioff, Phys. Rev. **119**, 324 (1960).

¹⁴P. J. Karol and J. M. Miller, Phys. Rev. **166**, 1089 (1968).

¹⁵T. Perggren and G. Jacob, Nucl. Phys. **47**, 481 (1963); A. Johansson and Y. Sakamoto, Nucl. Phys. **42**, 625 (1963).

¹⁶J. R. Grover and A. A. Caretto, Jr., Ann. Rev. Nucl. Sci. **14**, 51 (1964).

¹⁷W. D. Myers, Phys. Letters **30B**, 451 (1969).

¹⁸W. D. Myers and W. J. Swiatecki, Ann. Phys. (N.Y.) **55**, 395 (1969).

¹⁹F. M. Kiely, Ph.D. thesis, Carnegie Institute of Technology, 1967 (unpublished).

²⁰D. L. Morrison and A. A. Caretto, Jr., Phys. Rev. **127**, 1731 (1962).

²¹J. B. J. Read and J. M. Miller, Phys. Rev. **140**, B623 (1965).

²²G. Rudstam, P. C. Stevenson, and R. L. Folger, Phys. Rev. **87**, 358 (1952).

²³L. P. Remsberg and J. M. Miller, Phys. Rev. **130**, 2069 (1963).

²⁴S. Meloni and J. B. Cumming, Phys. Rev. **136**, B1359 (1964).

²⁵A. A. Caretto, Jr., Nucl. Phys. **A92**, 133 (1967).

Experimental Studies of the Neutron-Deficient Gadolinium Isotopes. II. Gd^{145m}

R. E. Eppley and Wm. C. McHarris

Department of Chemistry and Cyclotron Laboratory,† Department of Physics,
Michigan State University, East Lansing, Michigan 48823*

and

W. H. Kelly

Cyclotron Laboratory,† Department of Physics, Michigan State University, East Lansing, Michigan 48823

(Received 13 July 1970)

The $N=81$ isomer Gd^{145m} is characterized as having a half-life of 85 ± 3 sec and an $M4$ isomeric transition of 721.4 ± 0.4 keV. It also has a direct β^+/ϵ branch to the $h_{11/2}$ state at 716.1 keV in Eu¹⁴⁵. The intensity of this branch is 4.7% of the decay, implying a $\log ft$ of 6.2. The $M4$ transition probability is calculated and compared with the trends among other isomeric transitions in this region.

I. INTRODUCTION

Gadolinium isotopes cover a wide range of nuclear types, extending from permanently deformed nuclei to spherical single closed-shell nuclei at $N=82$. As a result, systematic studies of their decay properties and structures should prove quite rewarding, for here is one of the few regions in the nuclidic chart where one can follow trends in

nuclear states when moving from one extreme nuclear type to another. We have embarked recently on such a systematic study. The first paper in this series described the electron-capture decay of Gd¹⁴⁹, a nucleus that lies midway between the spherical and spheroidal regions.¹ On the neutron-deficient side of $N=82$ the Gd isotopes have not been very well characterized until quite recently, although their decays present some interesting